The Journal of Nutrition
Methodology and Mathematical Modeling

Absorption and Distribution Kinetics of the ^{13}C-Labeled Tomato Carotenoid Phytoene in Healthy Adults[1–4]

Nancy E Moran,[5] Janet A Novotny,[8] Morgan J Cichon,[6] Kenneth M Riedl,[5,6] Randy B Rogers,[9] Elizabeth M Grainger,[5] Steven J Schwartz,[5,6] John W Erdman Jr.,[9] and Steven K Clinton[5,7]*

[5]The Ohio State University Comprehensive Cancer Center, [6]Department of Food Science and Technology, and [7]The James Cancer Hospital and Department of Internal Medicine–Division of Medical Oncology, The Ohio State University, Columbus, OH; [8]Human Nutrition Research Center, USDA, Beltsville, MD; and [9]Department of Food Science and Human Nutrition and Division of Nutritional Sciences, University of Illinois, Urbana, IL

Abstract

Background: Phytoene is a tomato carotenoid that may contribute to the apparent health benefits of tomato consumption. Although phytoene is a less prominent tomato carotenoid than lycopene, it is a major carotenoid in various human tissues. Phytoene distribution to plasma lipoproteins and tissues differs from lycopene, suggesting the kinetics of phytoene and lycopene differ.

Objective: The objective of this study was to characterize the kinetic parameters of phytoene absorption, distribution, and excretion in adults, to better understand why biodistribution of phytoene differs from lycopene.

Methods: Four adults (2 males, 2 females) maintained a controlled phytoene diet (1–5 mg/d) for 42 d. On day 14, each consumed 3.2 mg ^{13}C-phytoene, produced using tomato cell suspension culture technology. Blood samples were collected at 0, 1–15, 17, 21, and 24 h and 2, 3, 4, 7, 10, 14, 17, 21, and 28 d after ^{13}C-phytoene consumption. Plasma-unlabeled and plasma-labeled phytoene concentrations were determined using ultra-HPLC–quadrupole time-of-flight-mass spectrometry, and data were fit to a 7-compartment carotenoid kinetic model using WinSAAM 3.0.7 software.

Results: Subjects were compliant with a controlled phytoene diet, consuming a mean ± SE of 2.5 ± 0.6 mg/d, resulting in a plasma unlabeled phytoene concentration of 71 ± 14 nmol/L. A maximal plasma ^{13}C-phytoene concentration of 55.6 ± 5.9 nM was achieved 19.8 ± 9.2 h after consumption, and the plasma half-life was 2.3 ± 0.2 d. Compared with previous results for lycopene, phytoene bioavailability was nearly double at 58% ± 19%, the clearance rate from chylomicrons was slower, and the rates of deposition into and utilization by the slow turnover tissue compartment were nearly 3 times greater.

Conclusions: Although only differing from lycopene by 4 double bonds, phytoene exhibits markedly different kinetic characteristics in human plasma, providing insight into metabolic processes contributing to phytoene enrichment in plasma and tissues compared with lycopene. This trial was registered at clinicaltrials.gov as NCT01692340. *J Nutr* 2016;146:368–76.

Keywords: phytoene, tomato, compartmental modeling, kinetics, carotenoid

Introduction

Phytoene is a colorless carotenoid found in tomatoes, which may contribute to observed epidemiologic associations correlating greater tomato intake with reduced risk of cancers and cardiovascular events (1–8). Like other carotenoids, phytoene is a scavenger of singlet oxygen-free radicals (9), inhibits lipoprotein oxidation (10), and demonstrates an array of bioactivities in preclinical studies associated with anticancer action (11–14). Furthermore, there is marked interest in the ultraviolet

[1] Supported by the NIH National Center for Complementary and Alternative Medicine (R21AT005166), The James Cancer Hospital's Bionutrition and Chemoprevention Fund (310684), The Ohio State University Center for Clinical and Translational Science (UL1TR001070), The Ohio State University Comprehensive Cancer Center and its Nutrient and Phytochemical Analytic Shared Resource (P30CA016058), and a Pelotonia Postdoctoral Fellowship (to NEM). Some carotenoid standards were donated by BASF SE, Ludwigshafen, Germany and DSM, Heerlen, Netherlands.
[2] Author disclosures: NE Moran, JA Novotny, MJ Cichon, KM Riedl, RB Rogers, EM Grainger, SJ Schwartz, JW Erdman Jr., and SK Clinton, no conflicts of interest. Neither Pelotonia nor The James Cancer Hospital's Bionutrition and Chemoprevention Fund were involved in the design, implementation, analysis, or interpretation of the data for this publication.
[3] The content is solely the responsibility of the authors and does not necessarily represent the official views of the National Center for Advancing Translational Sciences or the NIH.
[4] Supplemental Tables 1–4 and Supplemental Figure 1 are available from the "Online Supporting Material" link in the online posting of the article and from the same link in the online table of contents at jn.nutrition.org.
*To whom correspondence should be addressed. E-mail: Steven.Clinton@osumc.edu.

Manuscript received July 16, 2015. Initial review completed August 12, 2015. Revision accepted November 2, 2015.
First published online December 16, 2015; doi:10.3945/jn.115.220525.

B–absorbing properties of phytoene because it is deposited in skin and may contribute to photoprotection associated with tomato product consumption in humans (15).

Phytoene is the first carotenoid in carotenogenesis and is thus found in many carotenoid-containing fruits and vegetables (16, 17), with appreciable amounts (0.5–5 mg/serving) occurring in tomatoes, apricots, carrots, papaya, sweet peppers, and winter squash (16). In the United States, tomatoes are the second most consumed "vegetable" (18) after potatoes, with 31.1 lb (14.1 kg) of fresh and canned tomatoes consumed per capita in 2012. Tomatoes are assumed to be the major phytoene source for Americans. Although phytoene is not currently included on the USDA Nutrient Database (19), estimates of American intake can be based on the ratio of phytoene to lycopene in red tomatoes of 1:6, based on an analysis of commonly consumed tomato products (16). Thus, American phytoene intake is estimated to be 0.75–1.1 mg/d, with lycopene being 4.5–6.5 mg/d (20). This estimate corresponds with 2.0 mg phytoene/d reported in Luxembourg (17).

Phytoene in human liver, breast, and lung is found at concentrations similar to other major dietary carotenoids (lutein, α- and β-carotene, lycopene, and α- and β-cryptoxanthin) (16). These tissue sites are also those where tomato consumption is associated with reduced disease risk (2, 21, 22). However, phytoene tissue concentrations differ from those of structurally similar lycopene. Relatively higher concentrations of phytoene are found in the lung, liver, and skin when adjusted for intake (16). Phytoene circulates in primarily LDL and VLDL cholesterol fractions, whereas lycopene is primarily in LDL and HDL cholesterol fractions (23). Phytoene is hypothesized to be more bioaccessible/available than lycopene due to a lesser tendency to crystallize. This behavior is predicted due to the "bent" conformation and greater rotational bond freedom (flexibility) of the predominant geometric isomer in foods, 15-*cis*-phytoene. In contrast, the most common lycopene isomer in tomato is in the all-*trans* configuration, containing a long conjugated polyene chain, making it straight, rigid, and thus highly crystallizable (**Supplemental Figure 1**) (24). The hypothesis that *cis* isomerization improves bioavailability is supported by a recent report of the greater bioavailability of tetra-*cis*-lycopene compared with all-*trans*-lycopene from tomato juice (24). Together, differences between phytoene and lycopene tissue and lipoprotein distribution patterns, along with rodent biodistribution and short-term kinetic findings (25, 26), suggest kinetic differences in their bioavailability, tissue uptake, or metabolism. Overall, very little is known about human phytoene kinetics, making it difficult to propose mechanisms underlying tissue and lipoprotein distribution patterns and to rationally design clinical trials to study its bioactivity in humans.

Recent advances in tomato cell culture technology provide a source of highly enriched isotopically labeled carotenoids for kinetic studies in humans (27, 28). Physiologic compartmental modeling of tracer kinetics provides insights into bioavailability, the rates at which carotenoids are distributed to and cleared from tissues and blood, and estimated tissue pool sizes. Here we define phytoene kinetic parameters in humans employing ^{13}C-phytoene and address the hypothesis that the kinetic parameters of ^{13}C-phytoene differ from those reported for lycopene, explaining differences in plasma kinetics and tissue distribution patterns.

Methods

Participants. In brief, men and women between 21 and 70 y who were not taking carotenoid-containing dietary supplements were recruited by word of mouth. Adults meeting the following criteria for metabolic status and clotting ability at the enrollment visit were invited to participate: BMI (in kg/m^2) between 18 and 27 (inclusive), Eastern Cooperative Oncology Group status of 0, and normal kidney function, liver function, lipids, blood counts, and clotting times as assessed by standard clinical laboratory procedures. Exclusion criteria included a known allergy or intolerance to tomatoes, a history of nutrient malabsorption or metabolic disorders with special diet recommendations, uncontrolled hyperlipidemia (serum total cholesterol >200 mg/dL, HDL cholesterol >160 mg/dL, and TGs >200 mg/dL), being a current smoker, having a history of endocrine disorders other than diabetes or osteoporosis requiring hormone administration, use of medications that interfere with dietary fat absorption, or use of any complementary or alternative medication that may interfere with carotenoid absorption or metabolism. The study was approved by and conducted in compliance with the ethical standards of The Ohio State University Institutional Review Board (#2009C0104), and written informed consent was obtained from all subjects. The trial was registered at clinicaltrials.gov (NCT01692340).

Blood chemistry measurements. Serum samples were analyzed in singular in the Ohio State Clinical Research Center Analytical Laboratory using the Dimension Xpand Clinical Chemistry System (Siemens Medical Diagnostics). The analytical sensitivity was 3.0 mg/dL for HDL cholesterol, 5 mg/dL for LDL cholesterol, 50 mg/dL for total cholesterol, 15 mg/dL for TGs, 0.05 mg/dL for creatinine, 14 U/L for alanine transaminase, and 5 U/L for aspartate aminotransferase.

Study design and specimen collection. To establish steady-state absorptive and metabolic conditions, 2 male and 2 female subjects were asked to incorporate foods from a provided list to target a daily intake of 1–5 mg (inclusive) phytoene beginning 2 wk before consumption of the ^{13}C-phytoene test meal. Subjects tracked their phytoene intake from 7 fruit and vegetable categories (**Supplemental Table 1**) on a daily worksheet (**Supplemental Table 2**). The worksheets were developed based on available published food phytoene concentrations (16, 17). Phytoene concentrations were not available for 3 commonly consumed tomato food products (pico de gallo, salsa, and tomato soup), and therefore estimates were made based on the assumption that phytoene is generally present at one-sixth the concentration of the known lycopene concentration in these products (16). On day 0, fasted subjects reported to the Clinical Research Center, provided a baseline blood sample, and then consumed 3.1 mg ^{13}C-phytoene in 15.0 mL extra-light olive oil (Pompeian, Inc.) on one English muffin (Thomas' Original; Bimbo Bakeries) under subdued lighting within 5 min and then consumed a low-carotenoid breakfast (**Supplemental Table 3**) within the next 20 min. The low-carotenoid breakfast provided 29 g fat (including the olive oil dose carrier). The 3.1-mg ^{13}C-phytoene dose was selected as a physiologically relevant amount easily obtained from a 1-cup (243-g) serving of tomato juice or 1/2-cup (132-g) serving of a tomato-based marinara pasta sauce (16). Timing for blood draws began when the dose was completely ingested. Blood was drawn (21 mL) hourly for 15 h, then at 17, 19, 21, and 24 h postdosing. During the initial 24-h stay at the Clinical Research Center, subjects were provided with a morning snack, low-carotenoid lunch, dinner, and evening snack at 3, 6, 10, and 13 h after test meal consumption, providing a total of 1933 kcal for the day (Supplemental Table 3). Subjects resumed recording their compliance to the controlled, 1- to 5-mg phytoene/d diet from days 1–28 and, with exception to the dosing day, consumed a daily multivitamin providing ~100% of the US FDA Daily Value for most micronutrients (One Daily Multiple Plus Minerals; CVS Caremark) from enrollment to day 28. The daily multivitamin was provided to ensure sufficient micronutrient status across subjects and provided 50% of the Daily Value of vitamin A with 80% as retinyl acetate and 20% as β-carotene. Fasted subjects returned to the Clinical Research Center for single blood draws 2, 3, 4, 7, 10, 14, 17, 21, and 28 d after consuming the test meal. To assess potential toxicity, blood count and liver function assays were repeated on day 28. Adverse events or unintended effects were evaluated using the National Cancer Institute's Common Terminology Criteria for Adverse Events, version 4.0 by the study staff and were reported to the Ohio State University Institutional Review Board as appropriate.

^{13}C-phytoene biolabeling and isolation from tomato cell suspension cultures. ^{13}C-phytoene was produced from tomato cell suspension cultures using a previously described "^{13}C-loading and ^{13}C-labeling" approach (27) with several modifications. Liquid ^{13}C-glucose–containing carotenoid production growth medium was inoculated with "Ailsa Craig" *hp-1* tomato cells for a 7-d-long ^{13}C-loading phase, during which tomato cells incorporated available ^{13}C. These pretreated cells were used to inoculate fresh liquid ^{13}C-glucose–containing carotenoid production growth media, cultures were grown for 7 d, and then the phytoene desaturase inhibitor, norflurazon, was added as previously described (29). Cultures were grown another 11 d, and cells were harvested by vacuum filtration and stored at −80°C until phytoene isolation.

The carotenoid-containing fraction was isolated from tomato cells using a previously published, optimized extraction method for tomato cell culture carotenoids (30), which was scaled up 10 times. Pooled, filtered extracts were concentrated to dryness and stored under argon gas until isolation of phytoene by semipreparatory HPLC, described below.

Isolation of phytoene by semipreparatory HPLC photodiode array. Phytoene was isolated from the carotenoid-containing extract using a semipreparatory gradient HPLC method. The HPLC system was equipped with a photodiode array detector (PDA 2996; Waters), and separations were achieved using a Waters Sunfire Prep C18 OBD column (150 mm × 10 mm ID, 5-μm particle size) maintained at 30°C preceded by a C18 guard column. The carotenoid-containing extract was dissolved in 0.5 mL ethyl acetate, centrifuged, and injected, and a gradient elution method using 2 mobile phases (A: 90% acetonitrile, 10% water; B: 100% ethyl acetate) was used to separate phytoene from other lipophilic extract components. The gradient method was eluted at 10 mL/min and initiated with 25% B; transitioned to 45% B over 13 min, to 50% B over 7 min, and to 100% B over 3 min; and then instantaneously returned to 25% B and was held at 25% B for 4 min. The phytoene-containing eluent was collected and concentrated under reduced pressure, and phytoene was extracted from the concentrate using hexanes. Hexanes were removed from the fractions under reduced pressure and then a stream of argon, and the pooled, isolated ^{13}C-phytoene was stored at −80°C. All solvents were HPLC grade and were obtained from Fisher Scientific.

^{13}C-phytoene dose. On the morning of dosing, ^{13}C-phytoene was solubilized in extra-light olive oil by first dissolving in methylene chloride and mixing with olive oil, and methylene chloride was removed by evaporation under a stream of nitrogen with gentle heating (40°C), followed by brief exposure to reduced pressure on a lyophilizer. Solvent removal was confirmed gravimetrically. An aliquot of the ^{13}C-phytoene was reserved to be used for an external calibration curve for mass spectrometric analysis of plasma ^{13}C-phytoene concentrations. Biolabeling yielded a distribution of isotopologues (**Figure 1**). Based on mass spectrometric analysis of the dose using the ultra-HPLC–quadrupole time-of-flight-mass spectrometry system described below, >99.5% of the phytoene was ^{13}C-labeled, with 47% of the labeled phytoene present as the uniformly labeled isotopologue ($^{13}C_{40}H_{56}$), as determined by relative peak areas of the detectable isotopologues.

Extraction and ultra-HPLC–quadrupole time-of-flight-mass spectrometry analysis of plasma phytoene. Plasma ^{13}C-phytoene was extracted from plasma (1 mL) mixed with ethanol (1 mL) containing 0.1% butylated hydroxytoluene (wt:vol) with 5 mL of a hexane:ethanol:acetone:toluene solvent mixture (10:6:7:7; vol:vol:vol:vol) followed by sonication and centrifugation (2000 × *g*, 2 min at ambient temperature) for phase separation. The hyperphase was reserved and the hypophase was reextracted twice more. Pooled hyperphases were combined and solvent was removed under a stream of nitrogen. The analyses of plasma phytoene were conducted using an Agilent 1290 Infinity UHPLC System with a photodiode array detector coupled to an Agilent 6550 iFunnel Q-TOF-MS. The plasma extract was dissolved in 300 μL of 1:1 methyl *tert*-butyl ether:methanol, and 5 μL was injected onto an Agilent Zorbax Eclipse Plus C18 Rapid Resolution HD column (1.8 μm; 2.1 × 150 mm) maintained at 40°C. The gradient elution method consisted of 2 mobile phases (A: 60% methanol, 35% methyl *tert*-butyl ether, 5% water, 0.1% formic acid; B: 20% methanol, 78% methyl *tert*-butyl ether, 2% water, 0.1% formic acid), which were eluted at 0.6 mL/min, starting with 0% B for 6 min, then increasing to 100% B over 1 min, holding at 100% B for 2 min, and reequilibration at 0% B for 2 min. Ionization was achieved using atmospheric pressure chemical ionization operated in positive ion mode. MS parameters were optimized for the detection of phytoene and were as follows: sheath gas temperature, 500°C; drying gas temperature, 290°C; gas flow rate, 13 L/min; nebulizer pressure, 20 psig; Vcap, 3500 V; and corona current, 40 μA. Photodiode array and mass spectrometric data were

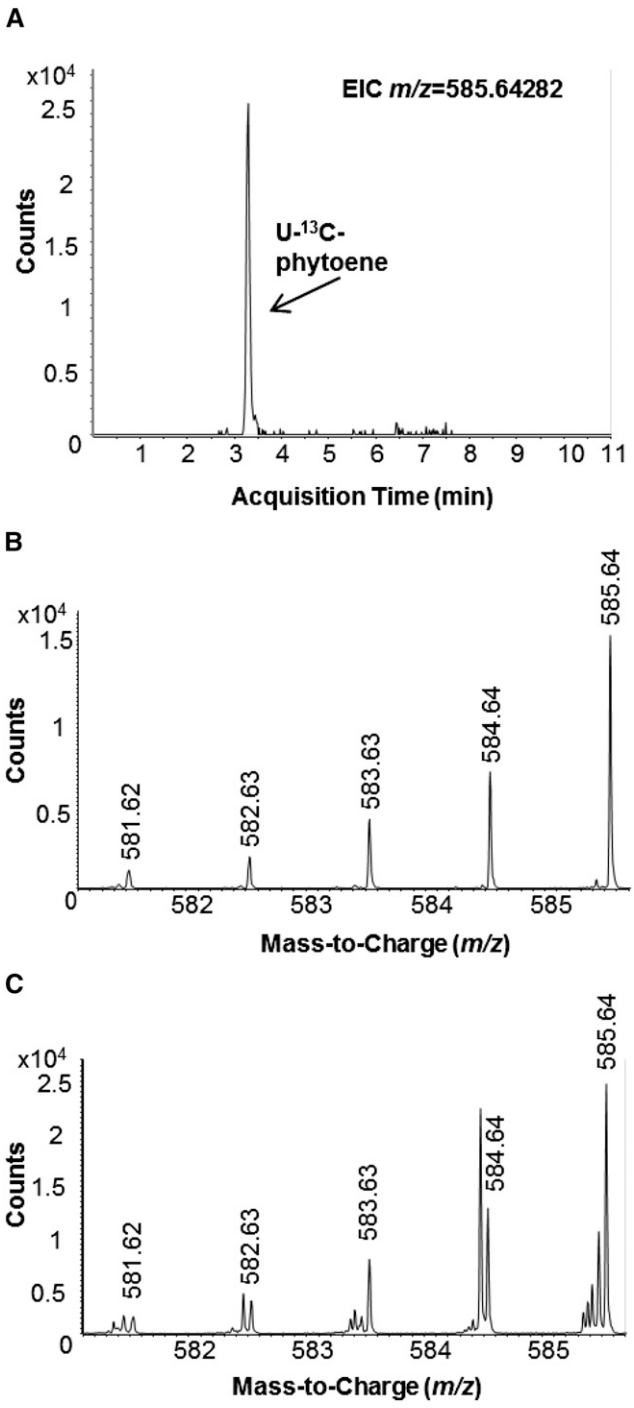

FIGURE 1 Mass chromatogram of ^{13}C-phytoene isolated from tomato cell suspension cultures (A) and mass spectra of most enriched mass isotopologues in the ^{13}C-phytoene dose (B) and in plasma of a subject after he consumed ^{13}C-phytoene (C). In the spectra, *m/z* 585.64 represents the uniformly labeled ($^{13}C_{40}H_{56}$) isotopologue, and each peak to the left represents a successively less-enriched isotopologue. EIC, extracted ion chromatogram.

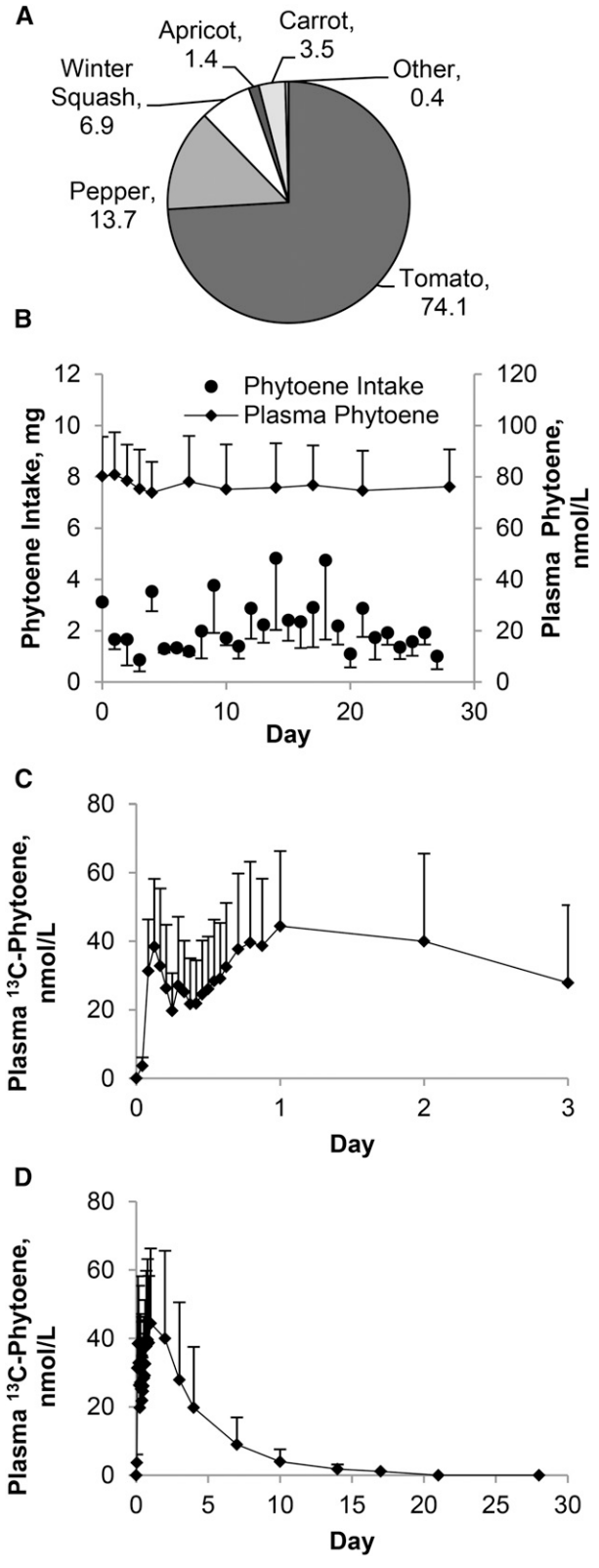

FIGURE 2 Percent contribution of recorded food categories providing dietary phytoene, during a 6-wk controlled phytoene dietary intervention (A), daily intake of phytoene recorded by subjects and resultant plasma unlabeled phytoene concentrations over 4 wk after ^{13}C-phytoene consumption (B), and the time-plasma ^{13}C-phytoene concentration curves over the first 3 d (C) and 28 d after ^{13}C-phytoene consumption (D). See Supplemental Table 1 for specific foods included in each category in panel (A); ''Other'' is the combined contributions of melons and citrus, because no papaya was consumed during the study period. Values in panel (A) are means, $n = 4$; values in panels (B–D) represent the means ± SEMs, $n = 4$.

acquired using Agilent MassHunter Data Acquisition software and analyzed using Agilent MassHunter Qualitative Analysis software. Plasma ^{13}C-phytoene concentrations were calculated from the extracted ion chromatogram peak area of ^{13}C-phytoene in plasma at the monoisotopic mass [$^{13}C_{40}H_{64}$; *m/z* 585.6428 $(M+H)^+$] using a ^{13}C-phytoene external calibration curve. Similarly, plasma unlabeled phytoene concentrations were calculated from the extracted ion chromatogram peak area of unlabeled phytoene at the monoisotopic mass [$C_{40}H_{64}$; *m/z* 545.5086 $(M+H)^+$] using a phytoene external calibration curve. The phytoene limit of quantitation was 1.15 nmol/L, and the limit of detection was 0.38 nmol/L.

Primary kinetic parameter estimation. The mean time of maximal plasma ^{13}C-phytoene concentrations and the mean maximal plasma ^{13}C-phytoene concentrations were calculated for the 4 subjects based on the observed data. The AUC of the time-plasma ^{13}C-phytoene concentration curves was calculated using the log-linear trapezoidal rule (31).

Physiologic compartmental model of phytoene kinetics. Plasma-unlabeled and plasma-labeled phytoene data were analyzed using a previously developed 7-compartment model for lycopene (28), a structurally similar tomato carotenoid, using WinSAAM modeling software (version 3.0.7). Physiologic compartmental modeling provides a means to noninvasively estimate the rate at which an analyte (in this case, phytoene) is exchanged between different physiologic compartments as well as to estimate the mass of analyte found within different compartments over time. A compartment can represent either a physically distinct pool of phytoene (i.e., plasma phytoene) or a pool of analyte found in multiple physical locations in the body for which all of the phytoene molecules display the same kinetic behaviors within a given time frame (i.e., a fast- or slow-turnover tissue pool of phytoene). The compartments in the model are "connected" by differential equations representing the rate of phytoene transfer between compartments. This rate of transfer is expressed as a fractional transfer coefficient (FTC), which represents the fraction of phytoene within a given compartment (J) transferred to another compartment (I) per unit time and is denoted as an L(I,J) in WinSAAM notation. Accordingly, the flow rate of phytoene between compartments is calculated by multiplying the FTC by the mass of phytoene in the donor compartment. The initial FTC estimates for the phytoene compartmental model were based on the FTCs for ^{13}C-lycopene and unlabeled lycopene kinetics in 8 healthy adults (28), with the exception that the FTC for chylomicron uptake from the plasma by the fast turnover tissue pool was based on chylomicron clearance in subjects consuming olive oil (32). In addition, a parallel model of tracee (unlabeled phytoene) kinetics was included, with data inputs for plasma unlabeled phytoene concentrations measured in collected plasma and steady-state intakes and compartmental phytoene masses calculated from the tracer model. The model parameters for each subject were then adjusted in physiologically meaningful ways until the predicted plasma phytoene concentrations were in accord with the experimentally measured unlabeled and labeled phytoene concentrations and the model resulted in predicted tissue phytoene masses that were physiologically plausible, based on the literature (16). A least squares fitting routine was used to determine the final values of model parameters to produce the closest fit between observed data and model prediction of plasma-labeled and plasma-unlabeled phytoene concentrations.

Results

Production of ^{13}C-phytoene from tomato cell suspension cultures. Using a 2-phase, ^{13}C-loading and ^{13}C-labeling tomato cell culturing strategy, 8.72 L of tomato cell suspension cultures were harvested, yielding 2.53 kg of biomass and 14.4 mg of ^{13}C-phytoene, which was >99.5% ^{13}C-labeled and 47% uniformly labeled, with each subsequent isotopologue decreasing in abundance by ~50% (Figure 1).

Subject characteristics and controlled diet compliance. Baseline subject anthropometric measures and blood lipid profile are summarized in **Supplemental Table 4**. Subjects were able to comply with the controlled phytoene diet, reporting a mean ± SEM phytoene intake of 2.5 ± 0.6 mg/d, with the group means ranging from 0.87 to 4.8 mg/d. Most dietary phytoene intake came from tomato products, followed by sweet bell peppers and winter squash (**Figure 2**). Tomato soup was the single greatest dietary source of phytoene, providing a mean of 22 mg to each subject over the 6-wk period, and the most frequently consumed source of phytoene was raw tomato, constituting 19% of phytoene-containing food servings (a mean of 10 servings · person^{-1} · 6 wk^{-1}), which provided 17 mg phytoene to each subject over the 6-wk period. These mean intakes resulted in mean native plasma phytoene concentrations of 71 nmol/L (ranging from 74 to 81 nmol/L) over the course of the 4-wk post–^{13}C-phytoene consumption (**Table 1**).

Noncompartmental kinetic parameters for ^{13}C-phytoene. Plasma ^{13}C-phytoene was first quantifiable 1 h after ^{13}C-phytoene consumption, and plasma concentrations reached an early maximum at 3 h and a later maximum at 24 h, which were nearly equivalent in magnitude (Figure 2). ^{13}C-phytoene was last quantifiable in all subjects on day 7 (or day 8 for one subject who had to provide blood on day 8 instead of day 7) and was last quantifiable in any subject 17 d after dosing (Figure 2). The plasma half-life, maximal concentration, and time of maximal concentration for ^{13}C-phytoene are presented in Table 1.

Compartmental model of phytoene kinetics. The previously established 7-compartment model of lycopene kinetics proved to be a good starting point for phytoene kinetic modeling (**Figure 3**), but to improve the statistical certainty of the models, one parameter constraint, for L(5,6), or recycling of phytoene from lipoproteins back to the fast turnover tissue phytoene compartment, was included to be 0.462 [fractional standard deviation (FSD) = 0.17], which is the fractional catabolic rate for LDL cholesterol in healthy individuals (33). However, to remain conservative and allow the modeling process to lead to novel phytoene kinetic data-based kinetic parameters, no other statistical constraints were placed on the model. This approach worked well for 3 subjects but did lead to some statistical uncertainty around the terms describing efflux of phytoene from the slow turnover pool to the lipoproteins L(6,7) and irreversible loss from the slow turnover phytoene compartment L(0,7) for 1 subject. Other than these parameters for 1 subject, all other

TABLE 1 Native phytoene plasma concentrations and noncompartmental, single-dose kinetics in human subjects after oral ingestion of ^{13}C-phytoene[1]

Native phytoene	Values
Plasma native phytoene, nM	
Baseline (day 0)	73.2 ± 14.2
Final (day 28)	74.3 ± 6.6
^{13}C-phytoene	
C_{max}, nM	55.6 ± 5.9
T_{max}, h	19.8 ± 9.2
AUC (0–672), nmol · h · L^{-1}	4900 ± 1060
$T_{1/2}$, d	2.3 ± 0.2

[1] Values are means ± SEMs, n = 4. C_{max}, maximal concentration; $T_{1/2}$, half-life; T_{max}, time of maximal concentration.

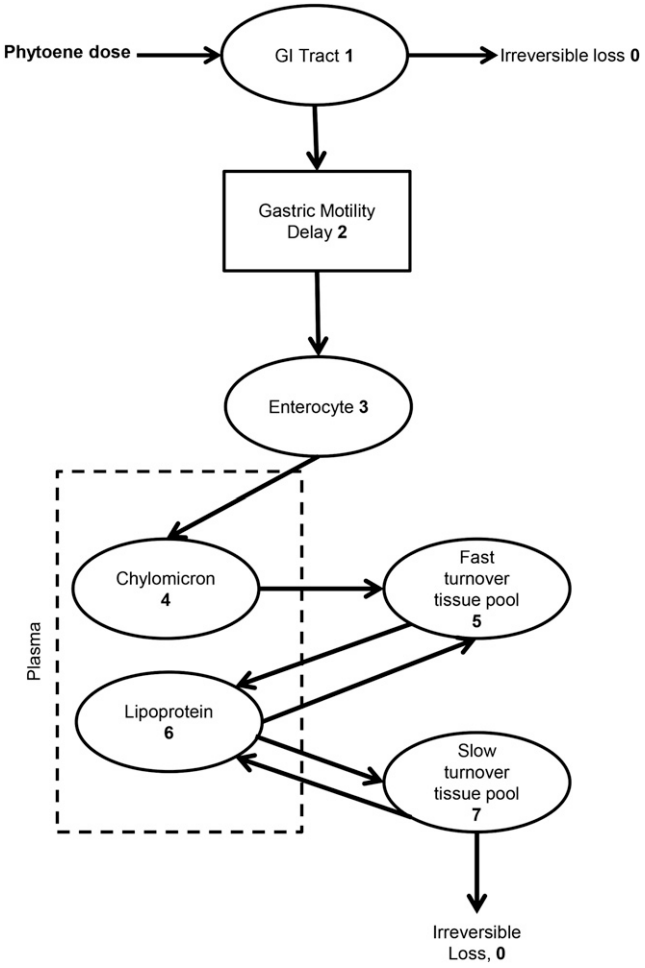

FIGURE 3 Compartmental pharmacokinetic model of phytoene absorption, distribution, and clearance. Arrows represent the mathematically modeled direction of phytoene exchange between compartments. Ovals represent compartments, or kinetically homogeneous pools of phytoene. The dashed line delineates the measured plasma compartment, but phytoene within lipoproteins and chylomicrons were not measured separately. The solid rectangle represents a delay element to account for interindividual variability in the time between ingestion and plasma appearance, likely correlating with gastrointestinal transit times. ^{13}C-phytoene tracer is introduced into compartment 1; bold numbers inside ovals represent the compartment number used in the compartmental analysis. GI, gastrointestinal.

subject parameters had low FSDs (≤0.6) and low correlation (≤0.8). The predicted model data fit the observed tracer and tracee data well (**Figure 4**). The proportion of the phytoene dose predicted to be in the plasma and tissue compartments over time is shown in Figure 4, as well as the model-predicted steady-state plasma phytoene mass over time. The plasma and fast-turnover tissue phytoene pools show an early peak at ~1.5 d, whereas the slow-turnover phytoene pool shows a peak phytoene mass occurring ~4 d after dose consumption, with phytoene clearance occurring at a slower rate from the slow turnover pool than from the fast turnover pool, as expected. The final population mean FTCs and intercompartmental phytoene flow rates for the 4 subjects are presented in **Table 2**, estimated phytoene masses in each compartment during steady-state feeding conditions are found in **Table 3**, and estimated gastrointestinal delay time, phytoene bioavailability, and steady-state phytoene intake are found in **Table 4**. For this initial ^{13}C-phytoene modeling effort, empirical data for LDL- or VLDL-associated phytoene was not

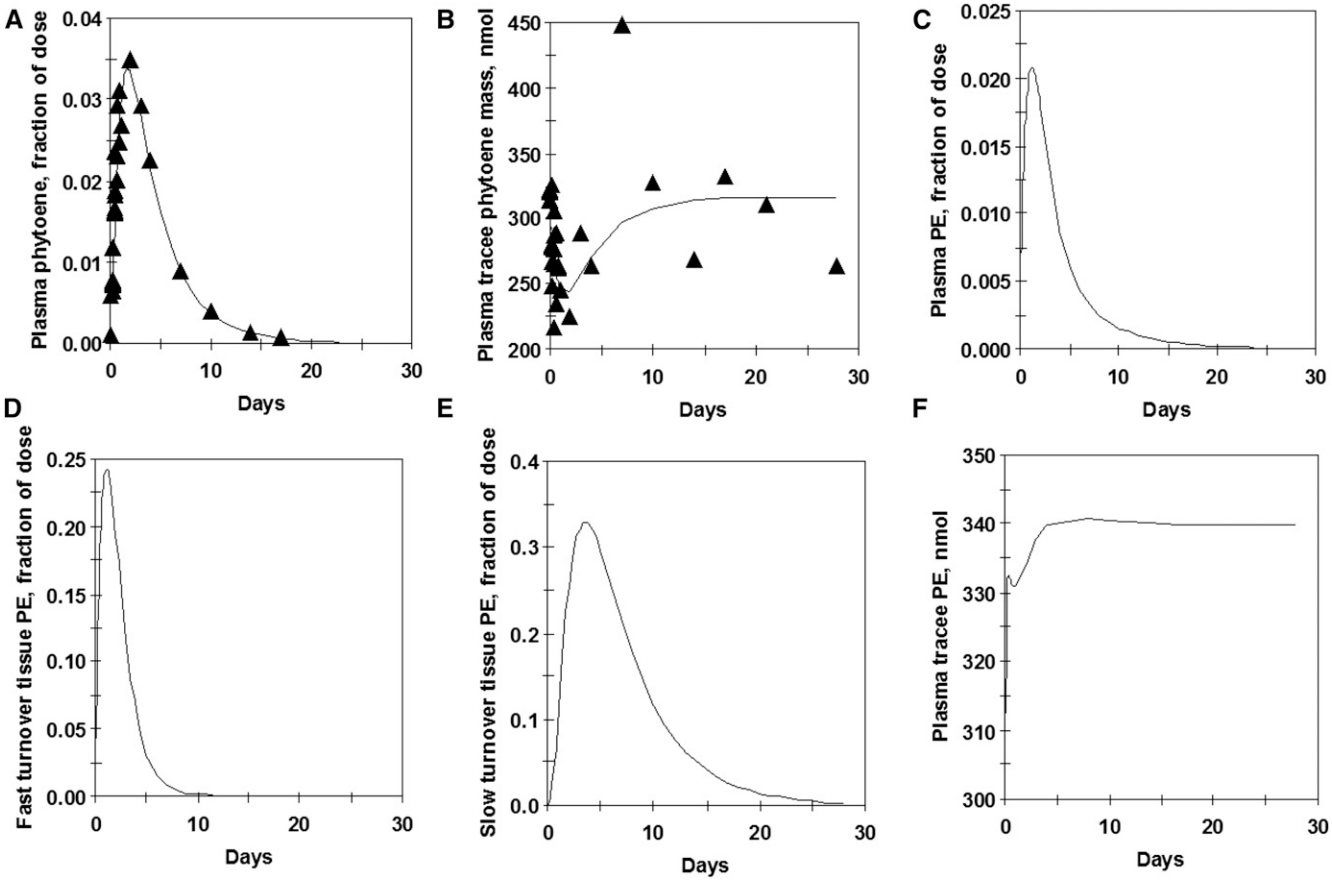

FIGURE 4 Model-predicted plasma (A, B) and tissue phytoene (C–E) plots over time. Examples of the fit of the observed to compartmental model-predicted data for plasma tracer phytoene concentrations (A) and plasma tracee (native) phytoene concentrations over 28 d (B) for 1 subject. Model calculated data based on population analysis of 4 subjects of the predicted fraction of ^{13}C-phytoene tracer dose in plasma (C), fast-turnover tissue phytoene compartment (D), slow-turnover tissue phytoene compartment (E), and the predicted level of plasma tracee phytoene in subjects consuming the controlled phytoene, steady-state diet (F). PE, phytoene.

incorporated in the model, and therefore the kinetics of phytoene as it is associated with different lipoprotein particle classes were not decisively characterized. However, because carotenes are known to be primarily associated with plasma lipoproteins, the physiologic processes underlying changes in plasma phytoene concentrations are understood to be the result of lipoprotein-tissue interactions, and in that way, the model and the data were interpreted in the context of lipoprotein kinetics.

Discussion

Phytoene is a commonly consumed and bioactive carotenoid that is readily accumulated in some tissues, yet little is known about its absorptive and distributive kinetics in humans. In this report, we used tomato cell suspension culture technology (27, 29, 34) to generate highly enriched, ^{13}C-phytoene to follow kinetics in humans. We also developed a novel phytoene scoresheet

TABLE 2 Compartmental kinetic parameters for model of phytoene disposition in human subjects after ^{13}C-phytoene consumption[1]

From donor compartment (compartment no.)	To recipient compartment (compartment no.)	Flow rate, nmol/d	Fractional transfer coefficient, d^{-1}
Gastrointestinal tract (1)	Irreversible loss (0)	3070 ± 2460	83.1 ± 37.8
Gastrointestinal tract (1)	Delay compartment (2)	1680 ± 430	117 ± 37.8
Delay compartment (2)	Enterocyte (3)	1680 ± 430	33.9 ± 2.21
Enterocyte (3)	Chylomicrons (4)	1680 ± 430	1.06 ± 0.201
Chylomicrons (4)	Fast-turnover tissue pool (5)	1680 ± 430	93.7 ± 16.2
Fast-turnover tissue pool (5)	Lipoproteins (6)	1760 ± 440	0.860 ± 0.179
Lipoproteins (6)	Fast-turnover tissue pool (5)	89 ± 20	0.390 ± 0.0443
Lipoproteins (6)	Slow-turnover tissue pool (7)	2680 ± 780	11.7 ± 2.69
Slow-turnover tissue pool (7)	Lipoproteins (6)	1010 ± 360	0.145 ± 0.0579
Slow-turnover pool of tissue phytoene (7)	Irreversible loss (0)	1680 ± 430	0.218 ± 0.0563

[1] Values are means ± SEMs, $n = 4$.

TABLE 3 Compartmental model-calculated steady-state phytoene masses in physiological compartments based on phytoene kinetics in human subjects after ^{13}C-phytoene consumption[1]

Compartment (no.)	Steady-state phytoene mass, nmol
Chylomicrons (4)	19 ± 4
Lipoproteins (6)	228 ± 43
Fast-turnover tissue phytoene pool (5)	2020 ± 95
Slow-turnover tissue phytoene pool (7)	9210 ± 2310

[1] Values are means ± SEMs, n = 4.

TABLE 4 Additional compartmental model-estimated parameters of phytoene kinetics in human subjects after ^{13}C-phytoene consumption[1]

Parameter	Estimate
Gastrointestinal delay, min	43.0 ± 2.8
Bioavailability, % absorbed	58.5 ± 18.9
Estimated daily intake of tracee	
nmol	4720 ± 2390
mg	2.57 ± 1.30

[1] Values are means ± SEMs, n = 4.

using available food phytoene concentration data to achieve steady-state phytoene intake and plasma concentration conditions in our subjects during the 42-d study duration. Furthermore, we defined the noncompartmental plasma kinetic parameters for phytoene. Using physiologic compartmental modeling, we found that the bioavailability of phytoene (58%) to be much greater than that of lycopene (23%) (28) and that several key FTCs for phytoene transfer into and out of tissue compartments markedly differed from that of lycopene, potentially explaining why phytoene is relatively enriched in many tissues, although it is less abundant in the diet than lycopene.

It is important to be able to control and monitor dietary intake of phytochemicals during clinical pharmacokinetic or pharmacodynamic studies. Using a dietary phytoene tracking worksheet, subjects were able to comply with the controlled phytoene diet (mean intakes within targeted 1–5 mg/d), resulting in similar day 0 baseline and day 28 plasma phytoene concentrations (Table 1 and Figure 2). Furthermore, this worksheet can be used for future clinical studies of bioactivity or kinetics that require controlled phytoene intakes.

The early time-concentration curve of phytoene shows a very rapid early increase in plasma phytoene concentrations to 3 h followed by a rapid drop and gradual increase up to 24 h after dosing (Figure 2). This differs from findings regarding lycopene and β-carotene, for which an early peak occurs between 6 and 12 h, depending on the amount consumed (28, 35, 36). The early peak likely corresponds with previous reports of early chylomicron and VLDL-associated phytoene release into the blood (24). The current compartmental modeling results indicate that greater bioavailability of phytoene combined with a slower clearance of chylomicron phytoene by the fast-turnover tissue pool (93 pools of phytoene/d compared with 173 pools of lycopene/d) may underlie a relatively greater early plasma phytoene response compared with lycopene. Different rates of clearance of chylomicron lycopene and chylomicron phytoene would indicate differential clearance of these carotenoids from the chylomicrons because the chylomicrons carrying the carotenoids are the same.

Phytoene has been hypothesized to be a more bioavailable carotenoid than lycopene. This is because phytoene is naturally found in a *cis* geometric conformation with relatively few conjugated double bonds and greater rotational freedom, keeping it in a noncrystalline form, which is thus more easily incorporated into mixed micelles in the gastrointestinal tract (24). Several previous observations support this hypothesis. First, relatively low concentrations (5.8 mg/d) of phytoene in tomato juice provided daily for 4 wk to healthy volunteers led to a nearly equivalent increase in plasma phytoene concentrations (0.19 μmol/L) as the change in plasma lycopene concentrations (0.17 μmol/L) in response to a much greater amount of lycopene (74.9 mg/d) in the juice (23). Second, although phytoene was a minor carotenoid (3% of total carotenoid) in tomato powder fed to gerbils for 4 wk and lycopene was the major carotenoid (93%), phytoene represented >30% of the plasma carotenoids (26). Also, a single dose of phytoene led to much greater increases in gerbil plasma phytoene concentrations at 6, 12, and 24 h (570%, 340%, and 650%, respectively) after dosing than a single lycopene dose (97%, 80%, and 39%, respectively) (26). However, none of these findings provide a true measurement of phytoene bioavailability. The current compartmental modeling estimates suggest that phytoene may be more bioavailable (58%) than lycopene (23%) (28). However, this result is confounded by the differing dose levels in these 2 studies, with 3.1 mg ^{13}C-phytoene being provided in the current study and 10.2 mg ^{13}C-lycopene being previously provided (28). It was previously shown that carotenoid bioavailability is inversely related to dose amount (37). Nonetheless, at this time, it appears that greater bioavailability could contribute to relatively enriched plasma concentrations of phytoene in humans and rodents compared with lycopene, but both absorptive and metabolic differences should be further investigated.

The plasma half-life of a compound permits determination of the frequency of consumption needed to attain a targeted plasma concentration and how long it would take to achieve steady-state conditions (31), both of which are key to rationally planning dietary interventions to assess kinetics and bioactivity. Interestingly, the current results suggest that the plasma half-life of phytoene (2.3 d) is less than half that of lycopene (6.2 d). This suggests that phytoene is not only more rapidly removed from plasma than lycopene but also that steady-state plasma phytoene concentrations may be achieved more rapidly with regular consumption than lycopene (31).

The plasma half-life of phytoene may be shorter than that of lycopene because phytoene is deposited into tissues more rapidly than the rate at which it is effluxed from tissues back into plasma, which may be due to either a greater rate of phytoene metabolism in the tissue or a slower transfer of phytoene from tissues back to lipoproteins. The compartmental modeling analyses suggest that both situations may be occurring, such that phytoene is more slowly effluxed from the fast-turnover tissue pool to lipoproteins (FTC = 0.86/d) than lycopene (FTC = 1.29/d), and phytoene is metabolically cleared >3 times as rapidly (FTC = 0.218/d) from the slow-turnover tissue pool than lycopene is (FTC = 0.061/d) (28). Slower efflux of phytoene than lycopene from tissues may reflect differences in cell membrane transporter affinity for these carotenoids. Findings have revealed that lycopene transport into cells is mediated by scavenger receptor class B, member 1 and CD 36 (38, 39), but the mechanisms of lycopene efflux from tissues and the mechanisms for phytoene uptake and efflux from cells remain unknown. Future studies of the differential affinities of proteins

involved in lipid transport for phytoene compared with lycopene will elucidate why the kinetics and biodistribution patterns of these 2 structurally similar, co-consumed carotenoids differ.

The rapid plasma half-life and the relatively fast rate of phytoene clearance from the slow-turnover tissue pool (mean ± SEM: 0.218 ± 0.056/d) indicates that a substantial amount of phytoene metabolites may be found in tissues soon after consumption of phytoene. However, the metabolism of phytoene is currently unknown, and thus there remain many questions regarding the identity of the metabolites produced and their potential to demonstrate bioactivity. However, in vitro and rodent ^{14}C-phytoene studies suggest that phytoene metabolites may occur in some tissues, such as the prostate (26, 40). Whether phytoene is a substrate for either the β-carotene oxygenase 1 or 2 carotenoid cleavage enzymes is unclear at this time. We previously reported lower hepatic phytoene concentrations in β-carotene oxygenase 1 knockout mice, possibly suggesting that compensatory overexpression of β-carotene oxygenase 2 in these mice could lead to greater rates of metabolism (41). To our knowledge, there is no conclusive identification of phytoene metabolites in human plasma, although such information would provide insight into the mechanisms by which phytoene is either enzymatically or nonenzymatically degraded before excretion. We and others speculate the cleavage products of non–provitamin A carotenoids may act as antagonists or agonists to multiple transcription factors within the steroid receptor superfamily, thereby affecting cell and tissue functions during health and disease (42, 43).

This describes the first compartmental model of phytoene kinetics. The compartmental modeling process used parallel models of plasma phytoene data for both the ^{13}C-labeled tracer and the unlabeled tracee pools. With these data, the mean ± SEM model-predicted daily phytoene intake was 2.57 ± 1.30 mg/d, which was in very good accordance with the subjects' reported daily intake of 2.5 ± 0.6 mg/d, thus enhancing our confidence in the model's accuracy. Although this study was small, being limited by the amount of ^{13}C-phytoene available, the kinetic parameters were defined with good statistical certainty (<0.6 FSD) and provide a framework for future studies of phytoene and carotenoid kinetics. Future phytoene kinetic modeling efforts could be strengthened by having larger group sizes, permitting a comparison of men and women as well as the inclusion of comprehensive human tissue phytoene concentration data from banked tissues. In addition, analysis of phytoene concentrations in plasma lipid fractions of the tracer-dosed individuals would allow for more precise modeling of the exchange of phytoene between tissues, chylomicrons, and lipoproteins.

In conclusion, this study applied stable isotope technology to define the noncompartmental and compartmental kinetic parameters of phytoene in humans and provides a foundation for planning and interpreting future studies on phytoene pharmacokinetics and dynamics. The strengths of the current study include the novel production and use of ^{13}C-phytoene for kinetic tracing in both men and women. In addition, the novel development of a system to control phytoene intake promoted steady-state absorptive and clearance conditions that were not likely to be perturbed by the tracer dose, making conclusions representative of steady-state phytoene kinetic processes. Future studies using ^{13}C-phytoene to study metabolism and the role of interindividual genetic variation in determining kinetic responses to phytoene will define how metabolic processes may affect phytoene bioactivity.

Acknowledgments

We thank Mary Ann Lila for providing laboratory space and equipment for ^{13}C-phytoene production from tomato cell cultures and Disha Gandhi for assisting in the isolation of ^{13}C-phytoene from tomato cell cultures. NEM, JAN, MJC, KMR, RBR, EMG, SJS, JWE, and SKC designed the research; NEM, JAN, MJC, KMR, RBR, and EMG conducted the research; NEM, RBR, and JWE provided essential reagents, or materials; NEM, JAN, MJC, KMR, SJS, JWE, and SKC analyzed the data; and NEM and JAN performed the statistical and mathematical modeling analyses; NEM, JAN, and SKC wrote the paper; and SKC had primary responsibility for final content. All authors read and approved the final manuscript.

References

1. Engelmann NJ, Clinton SK, Erdman JW Jr. Nutritional aspects of phytoene and phytofluene, carotenoid precursors to lycopene. Adv Nutr 2011;2:51–61.
2. Eliassen AH, Hendrickson SJ, Brinton LA, Buring JE, Campos H, Dai Q, Dorgan JF, Franke AA, Gao YT, Goodman MT, et al. Circulating carotenoids and risk of breast cancer: pooled analysis of eight prospective studies. J Natl Cancer Inst 2012;104:1905–16.
3. Zu K, Mucci L, Rosner BA, Clinton SK, Loda M, Stampfer MJ, Giovannucci E. Dietary lycopene, angiogenesis, and prostate cancer: a prospective study in the prostate-specific antigen era. J Natl Cancer Inst 2014;106:djt430.
4. Giovannucci E. A review of epidemiologic studies of tomatoes, lycopene, and prostate cancer. Exp Biol Med (Maywood) 2002;227:852–9.
5. Giovannucci E, Ascherio A, Rimm EB, Stampfer MJ, Colditz GA, Willett WC. Intake of carotenoids and retinol in relation to risk of prostate cancer. J Natl Cancer Inst 1995;87:1767–76.
6. Karppi J, Kurl S, Makikallio TH, Ronkainen K, Laukkanen JA. Low levels of plasma carotenoids are associated with an increased risk of atrial fibrillation. Eur J Epidemiol 2013;28:45–53.
7. Karppi J, Laukkanen JA, Makikallio TH, Kurl S. Low serum lycopene and beta-carotene increase risk of acute myocardial infarction in men. Eur J Public Health 2012;22:835–40.
8. Karppi J, Laukkanen JA, Sivenius J, Ronkainen K, Kurl S. Serum lycopene decreases the risk of stroke in men: a population-based follow-up study. Neurology 2012;79:1540–7.
9. Martínez A, Stinco CM, Melendez-Martinez AJ. Free radical scavenging properties of phytofluene and phytoene isomers as compared to lycopene: a combined experimental and theoretical study. J Phys Chem B 2014;118:9819–25.
10. Shaish A, Harari A, Kamari Y, Soudant E, Harats D, Ben-Amotz A. A carotenoid algal preparation containing phytoene and phytofluene inhibited LDL oxidation in vitro. Plant Foods Hum Nutr 2008;63:83–6.
11. Satomi Y, Misawa N, Maoka T, Nishino H. Production of phytoene, a carotenoid, and induction of connexin 26 in transgenic mice carrying the phytoene synthase gene crtB. Biochem Biophys Res Commun 2004;320:398–401.
12. Ben-Dor A, Steiner M, Gheber L, Danilenko M, Dubi N, Linnewiel K, Zick A, Sharoni Y, Levy J. Carotenoids activate the antioxidant response element transcription system. Mol Cancer Ther 2005;4:177–86.
13. Nishino H. Cancer prevention by carotenoids. Mutat Res 1998;402:159–63.
14. Hirsch K, Atzmon A, Danilenko M, Levy J, Sharoni Y. Lycopene and other carotenoids inhibit estrogenic activity of 17beta-estradiol and genistein in cancer cells. Breast Cancer Res Treat 2007;104:221–30.
15. Stahl W, Sies H. β-Carotene and other carotenoids in protection from sunlight. Am J Clin Nutr 2012;96:1179S–84S.
16. Khachik F, Carvalho L, Bernstein PS, Muir GJ, Zhao DY, Katz NB. Chemistry, distribution, and metabolism of tomato carotenoids and their impact on human health. Exp Biol Med (Maywood) 2002; 227:845–51.
17. Biehler E, Alkerwi A, Hoffmann L, Krause E, Guillaume M, Lair ML, Bohn T. Contribution of violaxanthin, neoxanthin, phytoene and phytofluene to total carotenoid intake: assessment in Luxembourg. J Food Compos Anal 2012;25:56–65.

18. USDA, Economic Research Service. Tomatoes and potatoes are the most commonly consumed vegetables. Food Availability Data. Washington (DC). [Internet]. September 16, 2013 [cited 2014 Jan 3]. Available from: http://www.ers.usda.gov/data-products/chart-gallery/detail.aspx?chartId=40452#.UsdCM_uzNkp.
19. USDA Agricultural Research Service. National Nutrient Database for Standard Reference Release 26. Beltsville (MD): National Agricultural Library; 2013.
20. USDA Agricultural Research Service. 2012. Total nutrient intakes: percent reporting and mean amounts of selected vitamins and minerals from food and dietary supplements, by family income (as % of federal poverty threshold) and age, What We Eat in America, NHANES 2009–2010 [cited 2015 Jul 16]. Available from: www.ars.usda.gov/ba/bhnrc/fsrg.
21. Ip BC, Wang XD. Non-alcoholic steatohepatitis and hepatocellular carcinoma: implications for lycopene intervention. Nutrients 2013;6:124–62.
22. Ito Y, Wakai K, Suzuki K, Tamakoshi A, Seki N, Ando M, Nishino Y, Kondo T, Watanabe Y, Ozasa K, et al. Serum carotenoids and mortality from lung cancer: a case-control study nested in the Japan Collaborative Cohort (JACC) study. Cancer Sci 2003;94:57–63.
23. Paetau I, Khachik F, Brown ED, Beecher GR, Kramer TR, Chittams J, Clevidence BA. Chronic ingestion of lycopene-rich tomato juice or lycopene supplements significantly increases plasma concentrations of lycopene and related tomato carotenoids in humans. Am J Clin Nutr 1998;68:1187–95.
24. Cooperstone JL, Ralston RA, Riedl KM, Haufe TC, Schweiggert RM, King SA, Timmers CD, Francis DM, Lesinski GB, Clinton SK, et al. Enhanced bioavailability of lycopene when consumed as cis-isomers from tangerine compared to red tomato juice, a randomized, cross-over clinical trial. Mol Nutr Food Res 2015;59:658–69.
25. Campbell JK, Engelmann NJ, Lila MA, Erdman JW Jr. Phytoene, phytofluene, and lycopene from tomato powder differentially accumulate in tissues of male fisher 344 rats. Nutr Res 2007;27:794–801.
26. Moran NE, Clinton SK, Erdman JW Jr. Differential bioavailability, clearance, and tissue distribution of the acyclic tomato carotenoids lycopene and phytoene in mongolian gerbils. J Nutr 2013;143:1920–6.
27. Moran NE, Rogers RB, Lu CH, Conlon LE, Lila MA, Clinton SK, Erdman JW Jr. Biosynthesis of highly enriched ^{13}C-lycopene for human metabolic studies using repeated batch tomato cell culturing with ^{13}C-glucose. Food Chem 2013;139:631–9.
28. Moran NE, Cichon MJ, Riedl KM, Grainger EM, Schwartz SJ, Novotny JA, Erdman JW Jr., Clinton SK. Compartmental and noncompartmental modeling of ^{13}C-lycopene absorption, isomerization, and distribution kinetics in healthy adults. Am J Clin Nutr. In press.
29. Engelmann NJ, Rogers RB, Lila MA, Erdman JW Jr. Herbicide treatments alter carotenoid profiles for ^{14}C tracer production from tomato (*Solanum lycopersicum* cv. VFNT cherry) cell cultures. J Agric Food Chem 2009;57:4614–9.
30. Lu CH, Engelmann NJ, Lila MA, Erdman JW Jr. Optimization of lycopene extraction from tomato cell suspension culture by response surface methodology. J Agric Food Chem 2008;56:7710–4.
31. Atkinson AJ, Huang S-M, Lertora JJL, Markey SP. Principles of clinical pharmacology. 3rd ed. San Diego: Elsevier;, 2012.
32. Park Y, Harris WS. Omega-3 fatty acid supplementation accelerates chylomicron triglyceride clearance. J Lipid Res 2003;44:455–63.
33. Langer T, Strober W, Levy RI. The metabolism of low density lipoprotein in familial type II hyperlipoproteinemia. J Clin Invest 1972;51:1528–36.
34. Engelmann NJ, Campbell JK, Rogers RB, Rupassara SI, Garlick PJ, Lila MA, Erdman JW Jr. Screening and selection of high carotenoid producing in vitro tomato cell culture lines for [13C]-carotenoid production. J Agric Food Chem 2010;58:9979–87.
35. Gustin DM, Rodvold KA, Sosman JA, Diwadkar-Navsariwala V, Stacewicz-Sapuntzakis M, Viana M, Crowell JA, Murray J, Tiller P, Bowen PE. Single-dose pharmacokinetic study of lycopene delivered in a well-defined food-based lycopene delivery system (tomato paste-oil mixture) in healthy adult male subjects. Cancer Epidemiol Biomarkers Prev 2004;13:850–60.
36. Novotny JA, Kurilich AC, Britz SJ, Clevidence BA. Plasma appearance of labeled beta-carotene, lutein, and retinol in humans after consumption of isotopically labeled kale. J Lipid Res 2005;46:1896–903.
37. Diwadkar-Navsariwala V, Novotny JA, Gustin DM, Sosman JA, Rodvold KA, Crowell JA, Stacewicz-Sapuntzakis M, Bowen PE. A physiological pharmacokinetic model describing the disposition of lycopene in healthy men. J Lipid Res 2003;44:1927–39.
38. Moussa M, Gouranton E, Gleize B, Yazidi CE, Niot I, Besnard P, Borel P, Landrier JF. CD36 is involved in lycopene and lutein uptake by adipocytes and adipose tissue cultures. Mol Nutr Food Res 2011;55:578–84.
39. Moussa M, Landrier JF, Reboul E, Ghiringhelli O, Comera C, Collet X, Frohlich K, Bohm V, Borel P. Lycopene absorption in human intestinal cells and in mice involves scavenger receptor class B type I but not Niemann-Pick C1-like 1. J Nutr 2008;138:1432–6.
40. Campbell JK, Rogers RB, Lila MA, Erdman JW Jr. Biosynthesis of ^{14}C-phytoene from tomato cell suspension cultures (*Lycopersicon esculentum*) for utilization in prostate cancer cell culture studies. J Agric Food Chem 2006;54:747–55.
41. Ford NA, Elsen AC, Erdman JW Jr. Genetic ablation of carotene oxygenases and consumption of lycopene or tomato powder diets modulate carotenoid and lipid metabolism in mice. Nutr Res 2013;33:733–42.
42. Erdman JW Jr, Ford NA, Lindshield BL. Are the health attributes of lycopene related to its antioxidant function? Arch Biochem Biophys 2009;483:229–35.
43. Sharoni Y, Linnewiel-Hermoni K, Zango G, Khanin M, Salman H, Veprik A, Danilenko M, Levy J. The role of lycopene and its derivatives in the regulation of transcription systems: implications for cancer prevention. Am J Clin Nutr 2012;96:1173S–8S.